Am J Transl Res 2024;16(4):1424-1441
www.ajtr.org /ISSN:1943-8141/AJTR0154883

Original Article

Low expression of ACOT13 predicts poor prognosis and immunotherapy outcome in ovarian cancer

Ting Xie, Tingting Liu, Lan Wu, Nianhua Yi

Department of Women's Health Care, Maternal and Child Health Hospital of Hubei Province, Wuhan, Hubei, China

Received December 10, 2023; Accepted April 8, 2024; Epub April 15, 2024; Published April 30, 2024

Abstract: Objective: Acyl-CoA thioesterase 13 (ACOT13) is involved in lipid biosynthesis, gene transcription, and signal transduction. We explored the potential of ACOT13 to predict ovarian cancer (OC) prognosis and patient immunotherapy responses. Methods: The Cancer Genome Atlas and Gene Expression Omnibus databases were used to extract raw data. To investigate the potential of ACOT13 as a prognostic and immunotherapeutic marker for OC, bioinformatic analyses were performed using the TIMER website, LinkedOmics database, and R software. We also explored the effects on the invasive ability of OC cells in vitro using a ACOT13 knockdown. Results: The expression of ACOT13 in OC was high and associated with a better prognosis. The expression of ACOT13 was also linked to immune cell invasion immunity-related gene expression. Additionally, immunotherapy was more effective in patients with high ACOT13 expression levels. Multiple critical signaling pathways were found to be involved in the role of ACOT13 in energy metabolism and cell mobility based on Gene Ontology and Kyoto Encyclopedia of Genes and Genomes analyses. OC cells invaded and migrated significantly more when ACOT13 was knocked down. Conclusion: High ACOT13 expression in OC is associated to a better OC outcome.

Keywords: Acyl-CoA thioesterase 13, ovarian cancer, immunotherapy, prognosis analysis, bioinformatics analysis

Introduction

Ovarian cancer (OC) is among the deadliest malignancies in gynecology, with a five-year survival rate of < 45% [1] and is the eighth cause of cancer-related death in women according to the World Health Organization [2]. Current diagnosis of OC relies on the International Federation of Gynecology and Obstetrics (FIGO) stage system and serum biomarkers [3, 4]. It has been found that these markers are not ideal for precisely predicting a patient's prognosis and curative effects [5-7]. Most patients with OC are diagnosed at an advanced stage [8]. To determine the optimal treatment for OC, it is imperative to identify novel gene signatures and biomarkers to help early diagnosis.

Acyl-CoA thioesterase 13 (ACOT13) is a member of the ACOT group of enzymes, which are associated with the regulation of lipid and glucose metabolism [9]. ACOT13 is abundantly expressed in the liver and oxidative tissues and colocalizes with mitochondria and acyl-CoA substrates of long-chain fatty acids [10, 11]. The ACOT13 protein binds to lipids within cells, maintaining fatty acyl-CoA balance and controlling complex lipid synthesis [12]. This demonstrates that ACOT13 plays an essential role in energy metabolism and may be involved in the regulation of tumor growth. However, the role of ACOT13 in OC has not been explored.

The tumor microenvironment is influenced by tissue-infiltrating immune cells (TIIC), which are closely related to tumor progression and outcome [13]. In malignant tumors, there is an increase in cytotoxic T cells and T helper cells [14]. High levels of B and T cells, along with cytotoxic T cells, infiltrate thymomas with better outcomes [15]. Immune monitoring has been reinstated in recent years by activating the immune response through various powerful chemotherapy and radiotherapy treatments [16]. Consequently, immunotherapy has become increasingly popular in cancer treatment [17, 18]. The identification of biomarkers that can predict immunotherapy response requires tremendous effort.

https://doi.org/10.62347/OIQB4997

In this study, we first assessed the differential expression of ACOT13 in OC and normal tissues. We used various bioinformatics tools to investigate the associations between ACOT13 expression, OC prognosis, and clinicopathology. Additionally, we investigated the relationship between ACOT13 and tumor immunity, including TIIC, immune-related genes, immune checkpoints, and tumor microenvironment. Furthermore, ACOT13 protein-protein interactions (PPI) were identified, and gene enrichment analysis was conducted to investigate their potential functions. Assays were conducted to assess cell invasion and migration in ACOT13 knocked down OC cells using colony formation, scratch wound healing, and Transwell assays. This study offers novel targets for the diagnosis, treatment, and prediction of OC, and sheds light on the function of ACOT13.

Materials and methods

Data acquisition

The Cancer Genome Atlas (TCGA) and Gene Expression Omnibus (GEO) public databases provide complete annotations of ACOT13 gene expression datasets. TCGA database (https://cancergenome.nih.gov/) was used to obtain the gene sequence data and clinical information of the patients. GSE18520, GSE91061, and GSE78220 datasets were downloaded from GEO (https://www.ncbi.nlm.nih.gov/geo/). The GSE18520 dataset included ten normal ovarian tissues and 53 OC tissues. Programmed cell death 1 ligand 1 (PD-L1) was administered to patients with melanoma or non-small cell lung cancer in GSE91061 and GSE78220.

Identification of differentially expressed genes

Based on TCGA database, the expression levels of ACOT13 were compared with the FIGO stage, histologic grade, lymphatic invasion, tumor residuals, and tumor status. Additionally, the GSE18520 dataset was used to verify the differential expression of ACOT13 and a boxplot was created using the R package "ggplot2" (version 4.0.3) [19].

Prognosis analysis of ACOT13 expression in ovarian cancer

The predictive value of ACOT13 in patients with OC was evaluated using Kaplan-Meier (KM) survival and receiver operating characteristic (ROC) curves. Using TCGA database, we analyzed the overall survival (OS), progression-free survival (PFS), and disease-specific survival (DSS) data to clarify the relationship between survival rates of patients with ACOT13 and OC. KM and log-rank tests were used for survival analysis, with survival curves plotted using the R packages "survivor" and "survminer". We used the survival package to conduct Cox analysis and the ggpubr and limma packages to determine the clinicopathological correlations [20]. A multivariate Cox regression analysis was performed to determine the items that should be plotted as columns. In R software, the "forestplot" package was used to display *p*-values, 95% confidence intervals, and hazard ratios [21]. A comprehensive analysis of ACOT13 and its association with prognostic and clinical factors, including age, residual tumor, and primary therapy outcomes, was conducted in this study. Based on the results of multivariate Cox proportional hazards analysis, nomograms were developed using R software and the "rms" package.

Gene set enrichment analysis (GSEA)

In GSEA, gene distributions in a predefined gene set were analyzed in phenotype tables ordered by gene distribution to determine their role in the definition of phenotypes. As part of our study, we used the R package cluster profile for GSEA [22]. The mRNA levels of ACOT13 were compared between the high- and low-expression groups to determine whether there were significant differences in their functions and pathways. The reference gene set used in this study was H.all.v7.2. symbols [23]; the gene matrix files belong to the Hallmarks gene sets from the human Molecular Signatures Database. Statistical significance was defined as a normalized enrichment score (NES) > 1, *p*-adjusted, and a false discovery rate < 0.2.

Gene ontology and pathway enrichment analysis

LinkedOmics (http://www.linkedomics.org/login.php) is a publicly accessible database of recombinant clinical data from 32 TCGA cancer types, including data from clinical proteomic analyses of tumors. Using LinkedOmics, we predicted the biological functions of ACOT13 in OC [24]. The GSEA method was used to com-

plete Kyoto Encyclopedia of Genes and Genomes (KEGG) pathway enrichment analysis and biological process Gene Ontology (GO) analysis. Further analysis using LinkedOmics was performed on the genes significantly associated with ACOT13.

Analysis of the correlation between ACOT13 and immune cell infiltration

The GSVA package in R was used to conduct single-sample GSEA (ssGSEA). To determine whether immune cells had infiltrated, enrichment scores were calculated using specific gene markers for each type of immune cell [25]. The correlation between ACOT13 mRNA expression and immune cell infiltration was evaluated using Spearman's and Pearson's correlation analyses.

The stromal and immune scores were calculated using ESTIMATE using the R packages "limma" and "estimate" [26]. The CIBERSORT analytical tool was used to determine the cell composition of OC tissues based on their gene expression profiles and ACOT13 expression data. To analyze the relationship between ACOT13 and tumor microenvironment or immune cell infiltration, the R packages "ggplot2", "ggpubr", and "ggExtra" were used [27].

Analysis of the correlation between ACOT13 and immunotherapy

Researchers at Genentech created a cohort of patients with urothelial carcinoma treated with PD-L1 (http://research-pub.gene.com/IMvigor210CoreBiologies) as part of IMvigor 210 [28, 29]. This dataset contains complete survival and follow-up data as well as immunotherapy effect information. The Deseq2 R package was used to normalize the raw count data.

Our analysis also included the expression data of chemokines, chemokine receptors, and major histocompatibility complexes, as well as the expression data of immunoinhibitory and immunostimulatory genes. The R packages ggplot2, immuneeconv, heatmap, limma, RColorBrewer, and reshape2 were used to assess co-expression of ACOT13 with these genes. The tumor immune dysfunction and exclusion (TIDE) algorithm was used to determine how the patient responded to immune checkpoint inhibitor treatment.

Correlation between ACOT13 and drug sensitivity

Correlation between ACOT13 and drug sensitivity was performed as previously described [31]. We gathered survival, clinicopathological, and RNA sequences associated with ACOT13 data and retained TGCA-recorded clinical sample information. The Pharmacogenomic Genomics Cancer Drug Sensitivity database was used to predict the ACOT13 OS-related chemotherapy responses in cancer samples (https://www.cancerrxgene.org/). The 50% maximal inhibitory concentration (IC50) of the samples was predicted using Ridge regression, and the accuracy of the prediction was assessed using the "Prophetic" R package [31]. We removed the "battle" among all solid tumors, as well as the batch effects of tissue type, and averaged out repeated gene expression [31].

Cell culture

OC cells were purchased from the Wuhan University Cell Storage Center (Wuhan, China). The cells were cultured in RPMI-1640 medium (Gibco) containing 10% fetal bovine serum (Gibco) and 100 U/mL penicillin and streptomycin (Gibco). The cells were then incubated at 37°C in a 5% CO_2 atmosphere.

Short hairpin RNA (shRNA) and transfection

shRNA targeting ACOT13 (shACOT13; targeting sequence: 5'-CGATATGAACATAACGTACAT-3') and a negative control construct were purchased from Sigma-Aldrich. Lipofectamine 2000 (Thermo Fisher Scientific) was used to transfect cells with shRNA plasmids. During transfection, puromycin was added to the medium containing the transfected cells.

Reverse transcription-quantitative polymerase chain reaction (RT-qPCR)

Total RNA was extracted from the cells using TRIzol (Thermo Fisher Scientific) according to the manufacturer's instructions. Following the manufacturer's instructions, we reverse transcribed the RNA to cDNA using the PrimeScript RT Reagent Kit (YEASEN). For gene quantification, SYBR Green Master Mix (YEASEN) was used in a LightCycler 480 (Roche). β-actin was used as an internal control for gene quantification.

Colony formation assay

To determine the proliferative ability of the OC cells, colony formation assays were performed after shACOT13 transfection. After 15 days of culture, a drop of crystal violet solution (Servicebio) was used to stain cells at a density of 500 cells/well. Colonies (diameter ≥ 100 μm) were counted microscopically.

Scratch-wound healing assay

Cells were seeded in 6-well plates. Once they reached confluence, a 1-mL pipette tip was used to make an indentation at the center of the wells. At 0, 24, and 48 h, scratch widths were examined and photographed under a light microscope.

Transwell cell invasion assay

Transwell plates pre-coated with Matrigel (BD Biosciences) were seeded with OC cells and incubated for 48 h. A microscopic image of the cells on the lower side of the filter was obtained after fixing with 4% paraformaldehyde for 30 min, staining with 0.1% crystal violet solution, and fixing with 4% paraformaldehyde for 30 min.

Statistics

Statistical analyses were performed as previously described [21]. The Wilcoxon test was used to analyze differences between groups. Kruskal-Wallis and one-way analysis of variance tests were used to analyze the differences between groups. Correlation tests were conducted using Spearman's analysis, and survival curves were created using log-rank and Kaplan-Meier tests. The "maftools" R package was used to examine mutations between various groups. To calculate the hazard ratios and their 95% confidence intervals (CIs), a univariate Cox regression model was used, and the comparison groups were considered statistically significant when $P < 0.05$. The R software (version 3.6.1) was used for data analysis.

Results

Differential expression of ACOT13 in normal and ovarian cancer tissues

By comparing data from TCGA (including 88 normal ovarian tissues and 427 OC tissues), GSE18520 (including ten normal ovarian tissues and 53 OC tissues), and TIMER online tool, ACOT13 was found to be significantly upregulated in OC tissues (**Figure 1A-C**, $P < 0.001$). Grade IV FIGO was associated with the lowest ACOT13 expression levels, whereas grade II FIGO was associated with the highest expression levels (**Figure 1D**). In addition, ACOT13 expression was negatively correlated with the histological grade, lymphatic invasion, residual tumor, and tumor status (**Figure 1E-H**, $P < 0.05$). The ROC curve results were reported as the area under the ROC curve (AUC) scores (**Figure 1I**).

Relationship of ACOT13 expression with OS, PFS, DSS, and DFS

We explored the potential of ACOT13 as a prognostic marker for OC by correlating its expression with OS, PFS, and DSS. High ACOT13 expression in patients with OC was associated with longer OS according to KM survival curves (**Figure 2A**, $P = 0.000366$). Furthermore, the PFS of patients with high ACOT13 expression was significantly longer than that of patients with low ACOT13 expression (**Figure 2B**, $P = 0.0213$). In addition, ACOT13-expressing OC patients had longer DSS (**Figure 2C**, $P = 0.000109$). In general, patients with OC and low ACOT13 expression have poor prognosis.

Correlation of ACOT13 expression with ovarian cancer on patient prognosis

According to the results of univariate Cox regression analysis, ACOT13 expression, age, residual tumor, and primary therapy outcomes were associated with OC prognosis (**Figure 3A**). Multivariate Cox regression analysis demonstrated that ACOT13 expression ($P = 0.024$), residual tumor ($P = 0.003$), and primary therapy outcomes ($P < 0.001$) were independent prognostic factors for OC (**Figure 3B**). A nomogram was constructed to provide quantitative guidelines for predicting the one- and three-year OS in patients with OC (**Figure 3C**). Furthermore, the nomogram accurately estimated the one-, three-, and five-year OS rates according to the calibration curves (**Figure 3D-F**). Time-dependent ROC analysis showed AUC values of 0.871, 0.664, and 0.704 at one, three, and five years, respectively, indicating a high predictive power (**Figure 3G-I**). Therefore, ACOT13 could be used as a diagnostic marker for OC.

Functional enrichment analysis of high and low ACOT13-expressing samples

OC samples were divided into two groups based on ACOT13 expression to examine the potential

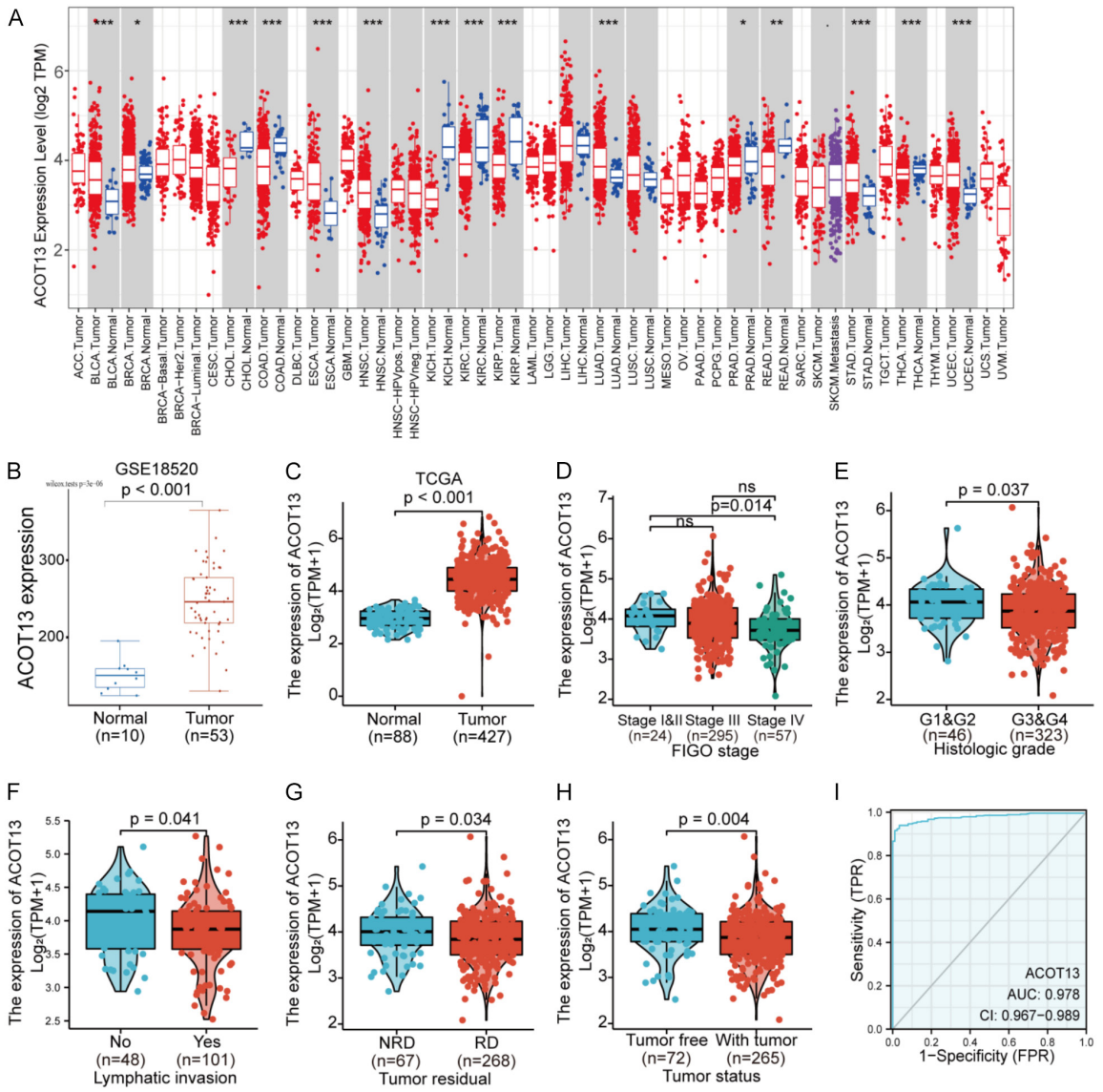

Figure 1. Differential expression of Acyl-CoA thioesterase 13 (ACOT13) in normal and ovarian cancer (OC) tissues. (A) ACOT13 expression in 33 types of cancers in TIMER website. (B) ACOT13 expression in normal and OC tissue in the GSE18520 datasets. (C) ACOT13 expression in normal and OC tissue in TCGA datasets. (D) Correlation between ACOT13 expression and the International Federation of Gynecology and Obstetrics (FIGO) stage of in OC. Association between ACOT13 expression and OC histologic grade (E), lymphatic invasion (F), tumor residual (G), and tumor status (H). (I) Receiver operating characteristic (ROC) curves analysis of ACOT13 in OC samples. *P < 0.05; **P < 0.01; ***P < 0.001.

mechanism by which ACOT13 suppresses tumor development. There were 348 differentially expressed genes (DEGs) that were highly expressed, whereas 124 DEGs were expressed at low levels (**Figure 4A**; selected threshold was |log2 (fold change)| > 1 and adjusted *P* < 0.05). Heatmaps were created to illustrate the correlation between ACOT13 expression trends and the top ten ACOT13 co-expression genes (**Figure 4B**). Additionally, we performed GSEA to identify ACOT13-related critical pathways. The most significant pathways were E2F targets (**Figure 4C**), G2M checkpoint (**Figure 4D**), MYC targets (**Figure 4E**), KRAS signaling DN (**Figure 4F**), spermatogenesis (**Figure 4G**), and pancreatic beta cells (**Figure 4H**).

PPI network, GO functional annotation, and KEGG pathway enrichment analysis of ACOT13

As shown in **Figure 5**, GeneMANIA and STRING databases were used to predict the interaction

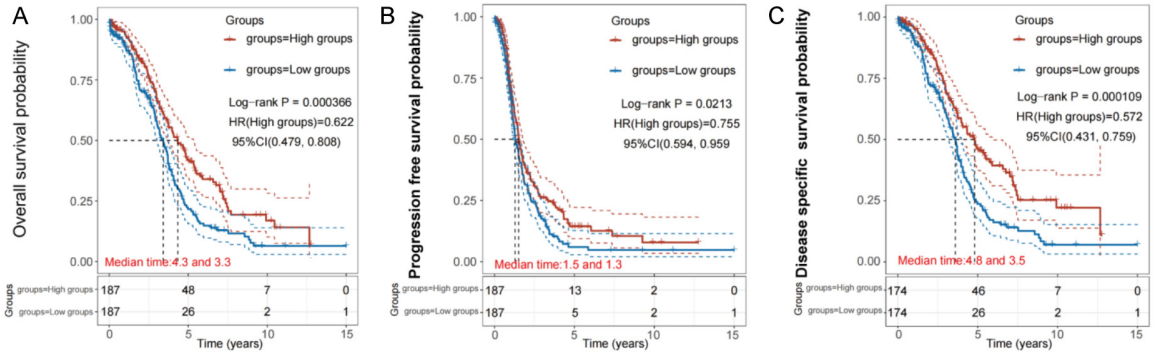

Figure 2. Relationship of ACOT13 expression with overall survival (OS), progression free survival (PFS), and disease specific survival (DSS). A. High ACOT13 expression groups had a longer OS. B. High ACOT13 expression groups had a longer PFS. C. High ACOT13 expression groups had a longer DSS. The upper and lower dashed lines are 95% confidence intervals.

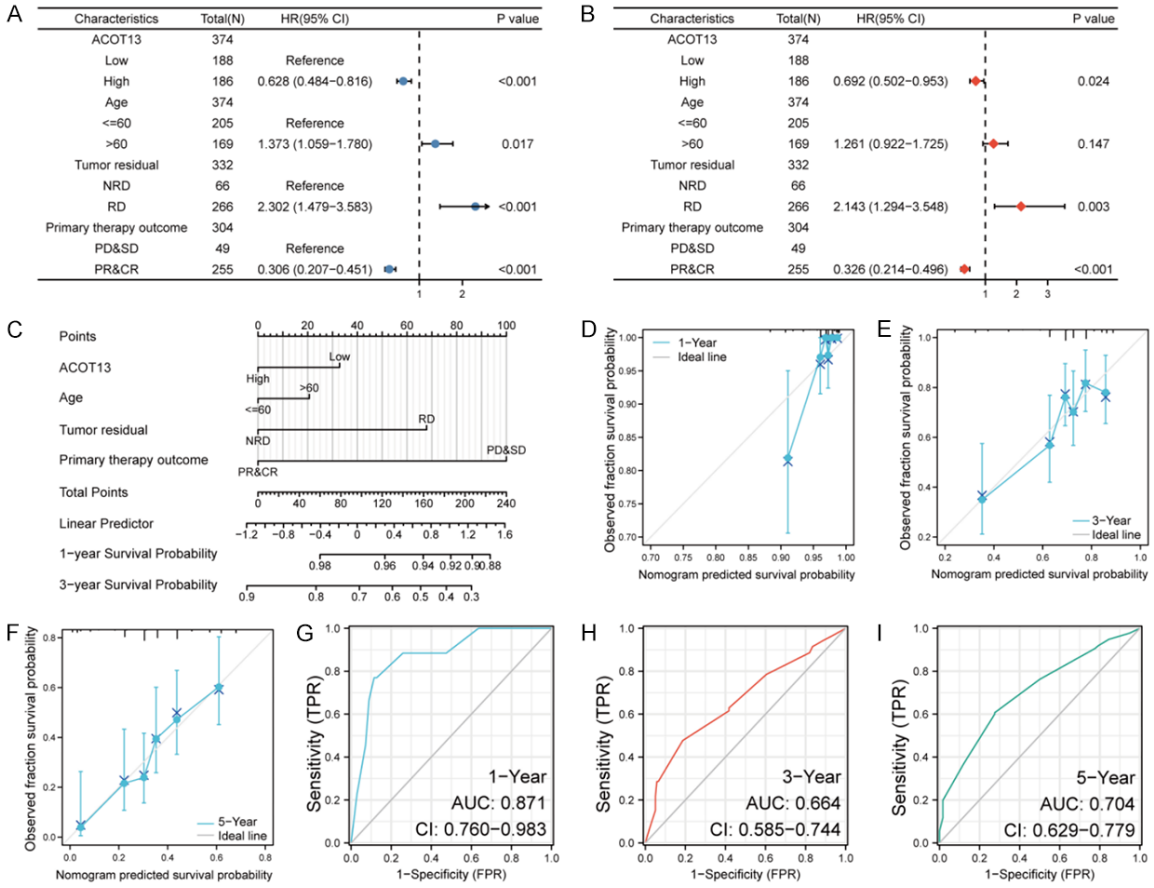

Figure 3. The predictive value of ACOT13 in OC. (A, B) Univariate and multivariate Cox regression was visualized in the forest plot. Nomogram (C) and calibration plots (D-F) Predict the 1-year, 3-year, and 5-year OS of OC patients. (G-I) The predictive ability for 1-, 3-, and 5-year prognosis with ACOT13 expression by time-dependent ROC curve analysis.

of the PPI network with ACOT13. Proteins interacting with ACOT13, identified using GeneMANIA, included THEM5, THEM7, THEM4, PCTP, ACOT7, ACOT12, and ACOT11 (**Figure 5A**). Proteins predicted to interact with ACOT13 using STRING included MCAT, ACOT9, ACOT1, ACOT12, PCTP, TDP2, ACOT11, and ACOT7 (**Figure 5B**).

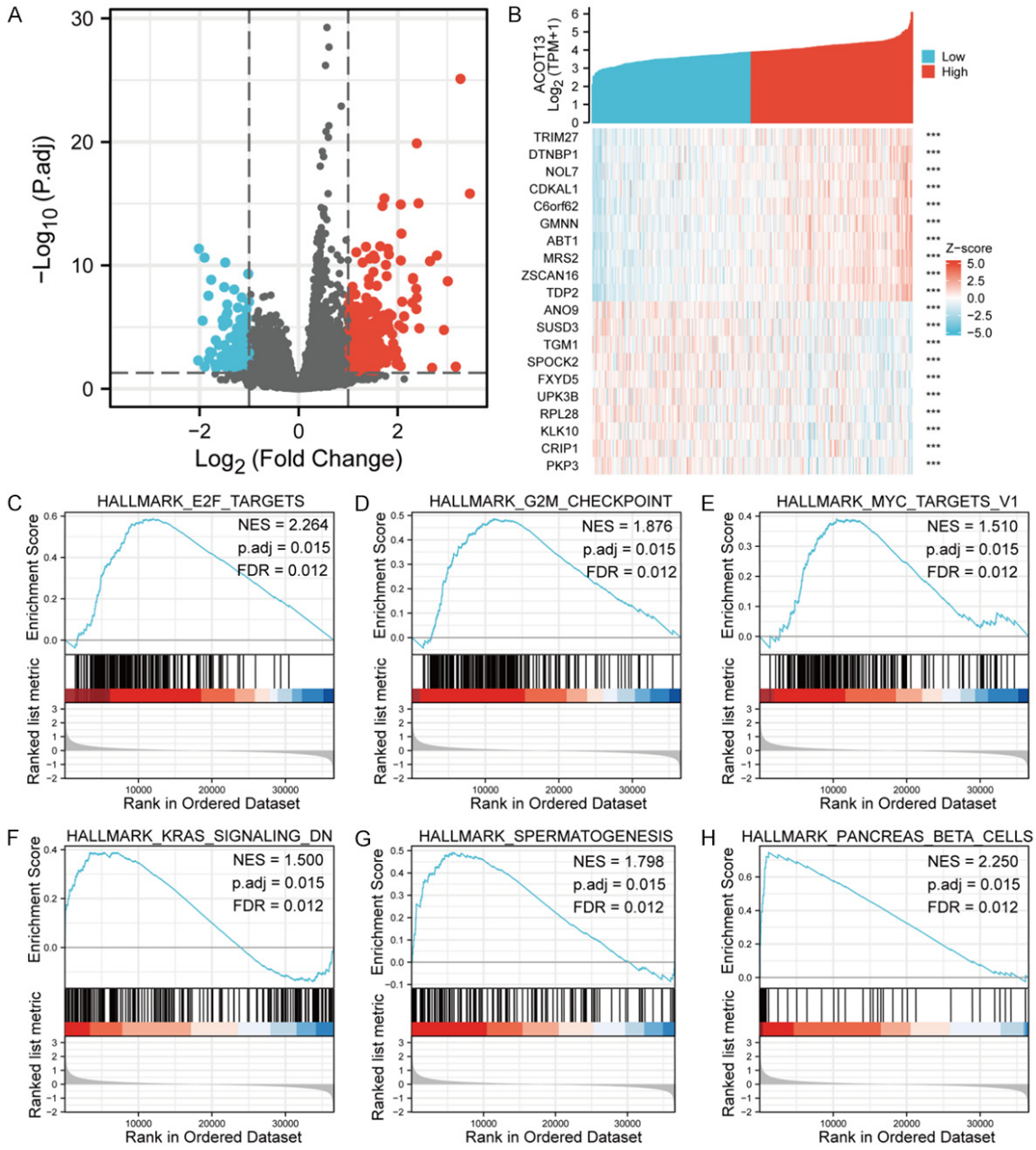

Figure 4. Functional enrichment analysis of ACOT13 in OC. (A) The volcano plot of differentially expressed genes (DEGs) was screened according to the expression level of ACOT13. (B) Heatmap of co-expression with ACOT13. Gene Set Enrichment Analysis (GSEA) was used to identify enriched gene classes associated with E2F targets (C), G2M checkpoint (D), MYC targets (E), KRAS signalling DN (F), spermatogenesis (G), and pancreas beta cells (H). ***P < 0.001.

Next, the potential function of ACOT13 in OC was analyzed using LinkedOmics. GO analysis of the biological processes (**Figure 5C**) indicated that ACOT13 was positively correlated with mitochondrial gene expression, mitochondrial respiratory chain complex assembly, NADH dehydrogenase complex assembly, tRNA metabolic processes, nucleoside triphosphate metabolic processes, protein transmembrane transport, ncRNA processing, and nucleoside monophosphate metabolic processes. In addition, ACOT13 was negatively correlated with neuronal projection guidance, epithelial cell development, vasculogenesis, and neuronal ensheathment. Moreover, GO analysis of cellular components indicated that the genes cor-

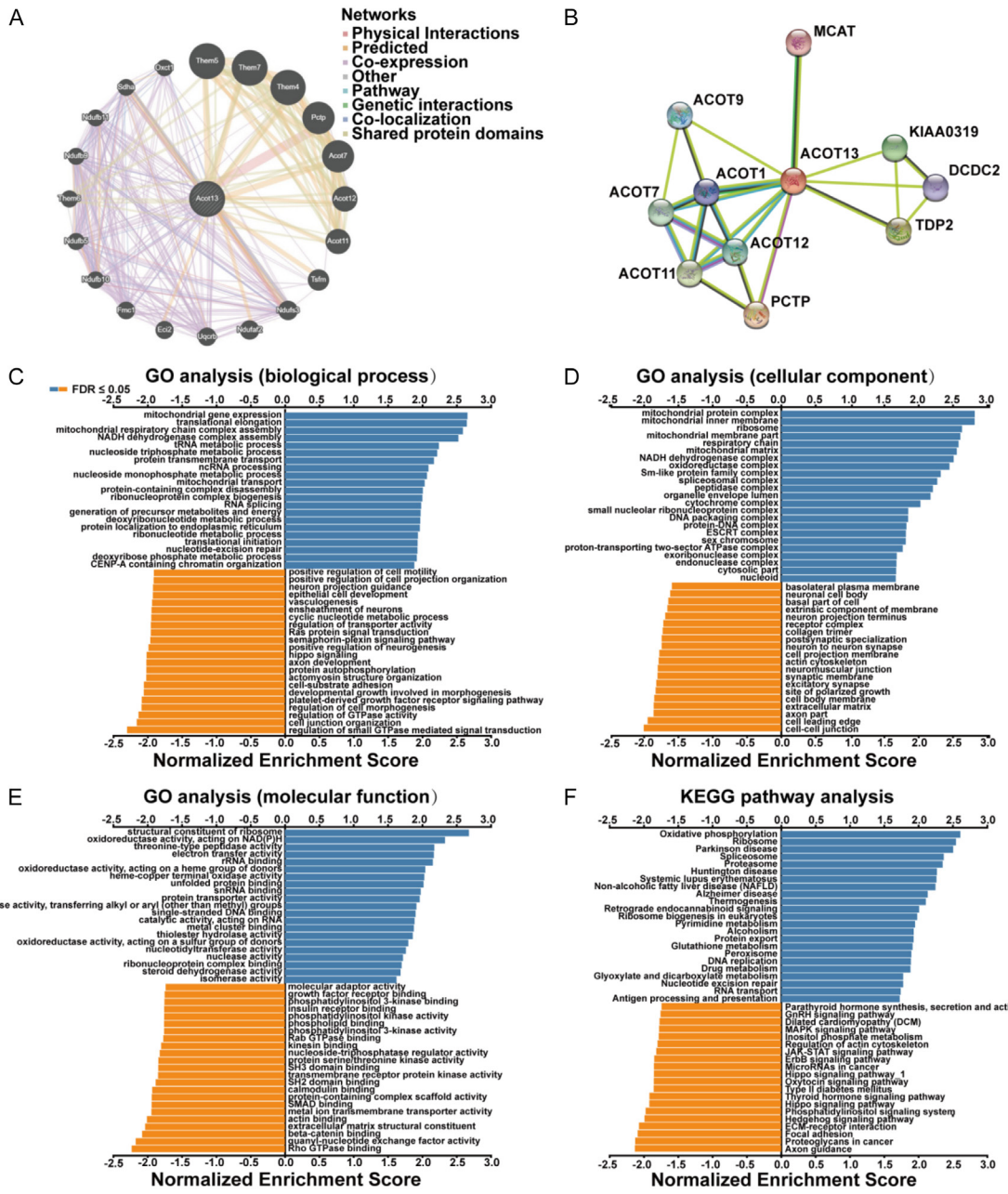

Figure 5. Protein-protein interaction (PPI) network, Gene ontology (GO) and Kyoto Encyclopedia of Genes and Genomes (KEGG) pathway enrichment analysis of ACOT13 in OC. PPI network of ACOT13 constructed from GeneMANIA databases (A) and STRING databases (B). GO analysis of the biological process (C), component (D), and molecular function (E) of ACOT13. (F) KEGG pathway analysis of ACOT13.

related with ACOT13 were mainly located in the mitochondrial protein complex, mitochondrial inner membrane, ribosome, mitochondrial membrane, and respiratory chain (**Figure 5D**). GO analysis of molecular function (**Figure 5E**) revealed that ACOT13 may function through the structural constituents of ribosomes, threonine-type peptidase activity, electron transfer activity, and rRNA binding. KEGG pathway analysis (**Figure 5F**) also indicated that ACOT13 was positively correlated with the processes of oxidative phosphorylation, ribosome, spliceosome, proteasome, DNA replication, drug metabolism, and RNA transport, and was negatively associated with the processes of cell mobility, epithelial cell development, GnRH,

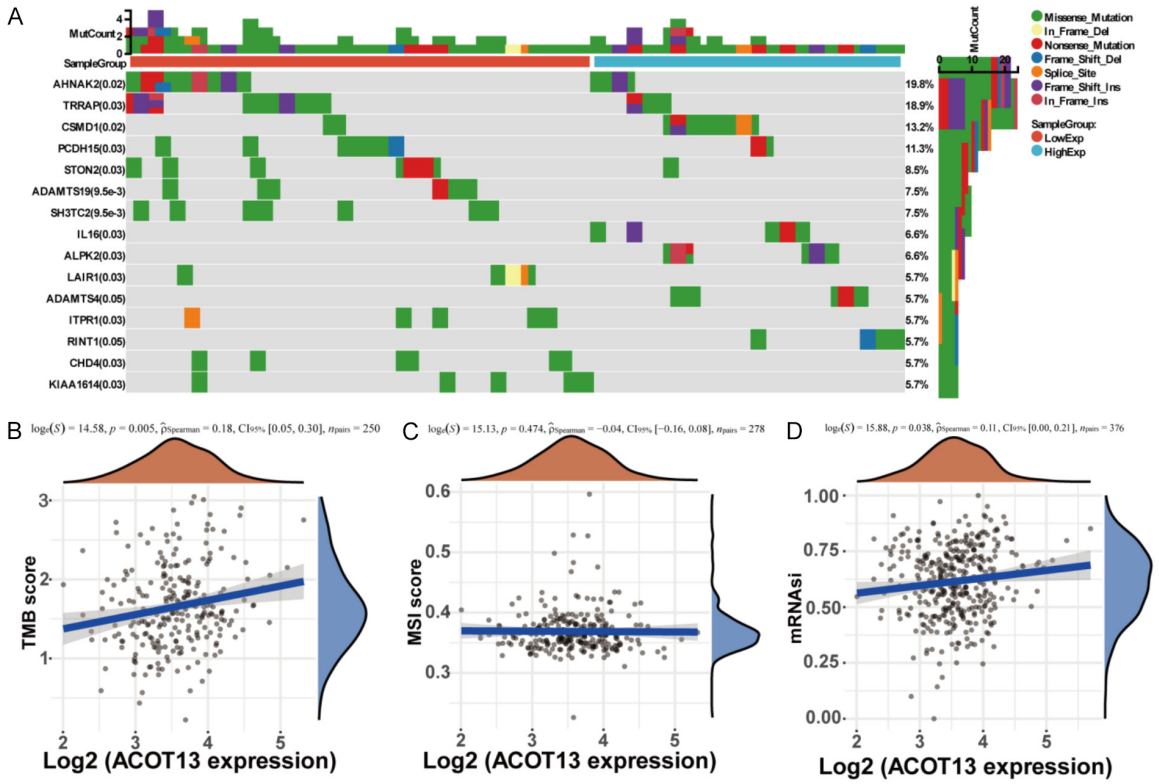

Figure 6. Landscape of mutation profiles in OC samples. (A) Mutation information of each gene in each sample was shown in the waterfall plot, with various color annotations to distinguish different mutation types. The barplot above the legend exhibited the mutation burden, and the other barplot on the right showed the distribution of mutation types among the top 15 genes. The correlation between ACOT13 expression and tumor mutation burden (TMB) (B) score and microsatellite instability (MSI) (C) score. (D) The correlation between ACOT13 expression and mRNA expression (mRNAsi) score.

MAPK, JAK-STAT, Hippo, and thyroid hormone signaling pathways.

Landscape of mutation profiles in ovarian cancer samples

To analyze and visualize the landscape of mutation profiles among OC patients, mutation data were downloaded from the TCGA database and the "maftools" R package was implemented. Waterfall plots displayed different mutation types for each sample, with various colors representing different mutations (**Figure 6A**). Most tumor-related mutations are missense. Moreover, the tumor mutation burden (TMB) and microsatellite instability (MSI) play important roles in tumor immunity. ACOT13 expression was positively correlated with the TMB score (**Figure 6B**, $P = 0.005$) and unrelated to the MSI score (**Figure 6C**, $P = 0.474$). In addition, ACOT13 expression positively correlated with the stemness index based on the mRNA expression score (**Figure 6D**, $P = 0.038$).

Correlation of ACOT13 expression with ovarian cancer immune cell infiltrates

To better understand how ACOT13 expression affects immune cell infiltration, we divided the ACOT13 high and low expression groups using the ESTIMATE algorithm scoring system. A significant negative correlation was observed between ACOT13 expression and the stromal, immune, and ESTIMATE scores (**Figure 7A-C**). To better understand the role of ACOT13 in OC, ssGSEA was used to examine the relationship between ACOT13 mRNA expression and immune cell infiltration. The correlation between infiltration of the 24 immune cells and ACOT13 expression is shown in **Figure 7D**. Further assessment of the cellular composition of TIIC in OC was performed using CIBERSORT. This suggested a statistically significant differ-

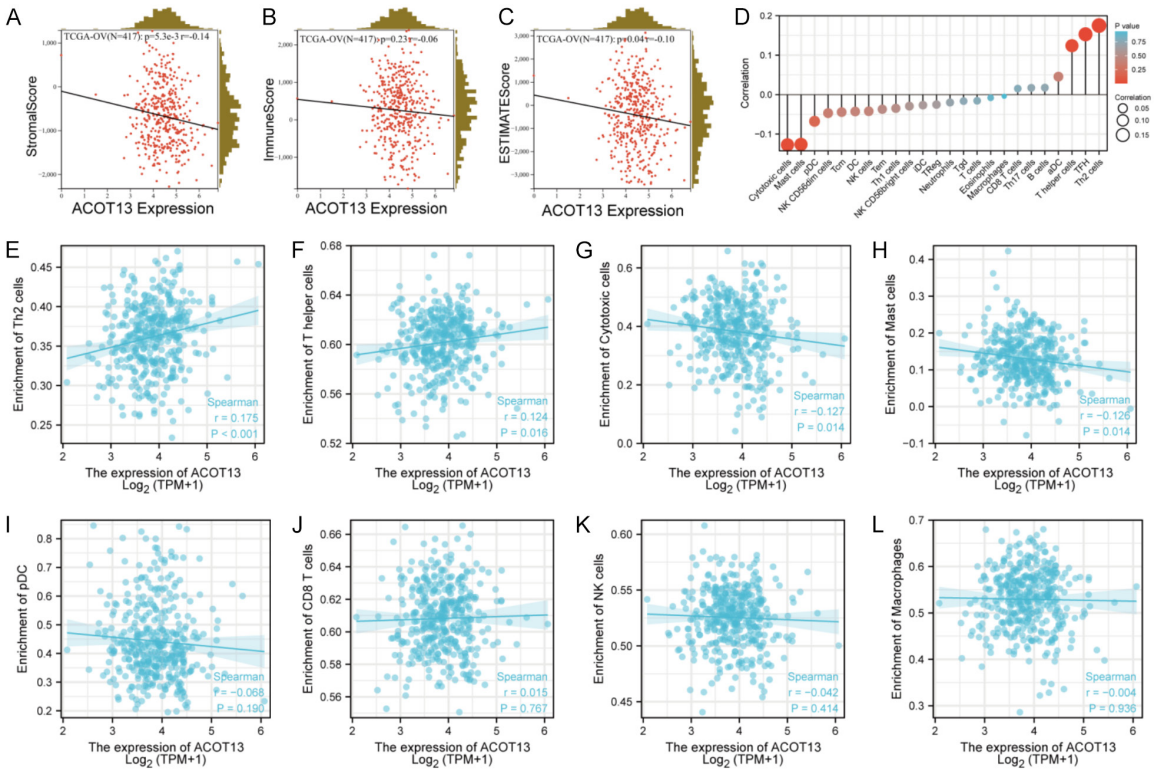

Figure 7. Correlations of ACOT13 expression with TIIC infiltration level in OC. Correlation of ACOT13 with stromal score (A), immune score (B) and ESTIMATE score (C) in OC. (D) Correlation between immune cell infiltration and ACOT13 expression utilized single-sample GSEA (ssGSEA). ACOT13 expression correlated with the immune infiltration of Th2 cells (E), T helper cells (F), cytotoxic cells (G), mast cells (H), plasmacytoid dendritic cells (I), CD8 T cells (J), natural killer cells (K), and macrophages (L).

ence between ACOT13 and Th2, T helper, cytotoxic, and mast cells ($P < 0.05$) (**Figure 7E-L**). According to these results, ACOT13 was critical for regulating TIIC infiltration into OC cells.

Relationship between the ACOT13 expression and the effect of immunotherapy

Immunotherapy for OC relies heavily on the anti-PD1/PD-L1 therapy. To demonstrate the connection between the expression of ACOT13 and immunotherapy effectiveness, we examined a treatment group (IMvigor210) that received anti-PD1/PD-L1 antibodies with extensive clinical information and a significant number of participants. Next, the IMvigor210 participants were categorized into groups based on their ACOT13 expression levels. The outlook of the groups varied slightly (**Figure 8A**, $P = 0.063$); however, individuals with high ACOT13 expression exhibited a more favorable complete response (CR)/partial response (PR) rate and a reduced SD/PD rate (**Figure 8B**, **8C**, $P < 0.05$). Next, we validated the immunotherapy efficacy prediction of ACOT13 expression using GSE91061 and GSE78220 datasets. The results indicated that high ACOT13 expression was associated with a better prognosis and a more effective response to immunotherapy (**Figure 8D-G**).

In addition, OC samples obtained from TCGA repository were categorized into ACOT13-low and ACOT13-high groups based on the expression of ACOT13. The immune checkpoint gene, SIGLEC15, was overexpressed in patients with high ACOT13 expressing patients with OC (Supplementary Figure 1, $P < 0.001$). Furthermore, we assessed the association between ACOT13 expression and immunotherapy response in patients with OC. ACOT13 expression was positively associated with lower TIDE scores in patients with high ACOT13 expression; however, this association was not statistically significant (Supplementary Figure 1). The relationship between ACOT13 and drugs commonly used in OC was also evaluated. The results showed that the expression of ACOT13

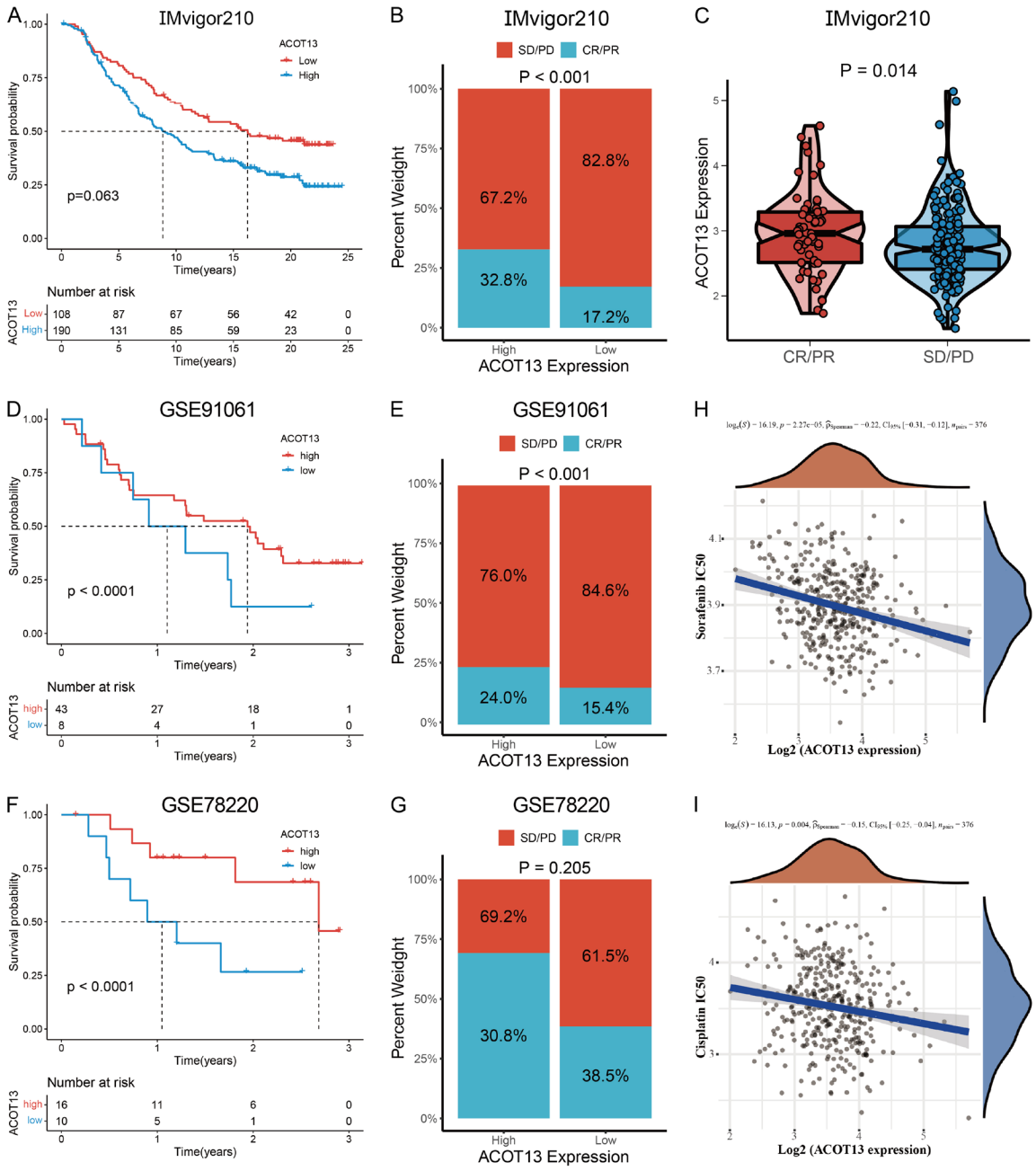

Figure 8. The role of ACOT13 expression in immunotherapy. (A) Kaplan-Meier plot of overall survival by ACOT13 expression groups for patients in the IMvigor210 cohort. (B) Proportions of immunotherapy response in high and low ACOT13 expression groups in the IMvigor210 cohort. (C) ACOT13 expression in different immunotherapy responses in the IMvigor210 cohort. (D) Kaplan-Meier plot of overall survival by ACOT13 expression groups for patients in the GSE91061 dataset. (E) Proportions of immunotherapy response in high and low ACOT13 expression groups in the GSE91061 dataset. (F) Kaplan-Meier plot of overall survival by ACOT13 expression groups for patients in the GSE78220 dataset. (G) Proportions of immunotherapy response in high and low ACOT13 expression groups in the GSE78220 dataset. Correlations ACOT13 with the IC50 of chemotherapy drugs, including Sorafenib (H) and Cisplatin (I). PR, Partial Response; PD, Progressive Disease; SD, Stable Disease; CR, Complete Response.

correlated with the efficacy of sorafenib (**Figure 8H**, $P < 0.001$) and cisplatin (**Figure 8I**, $P = 0.004$). Based on these findings, it is possible to predict the efficacy of immunotherapy using ACOT13 expression.

Co-expression of ACOT13 with immune-related genes in OC

Subsequently, ACOT13 gene expression correlated with immune-related genes. OCs express

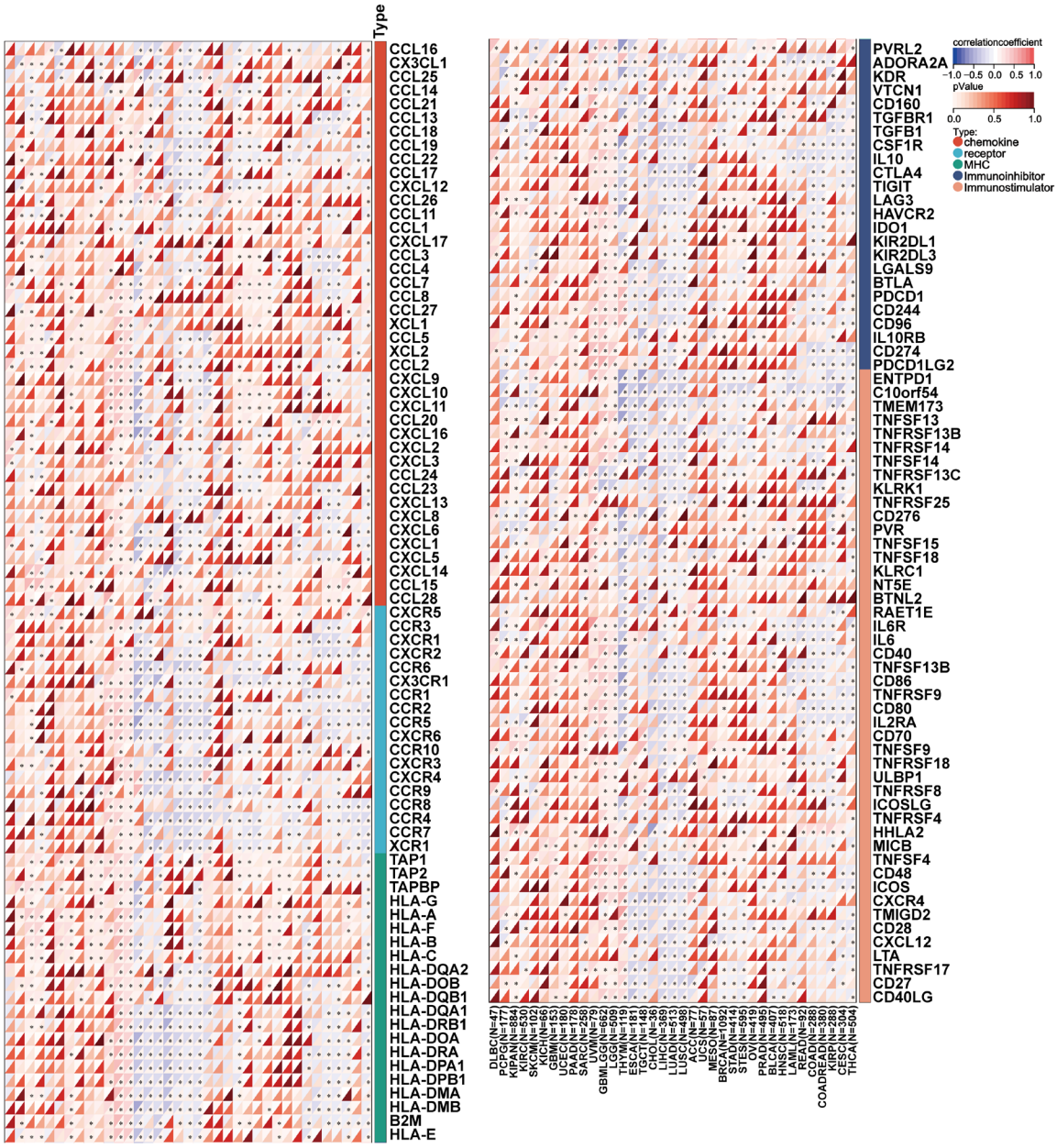

Figure 9. Pan-cancer analysis of the correlation between ACOT13 expression and immune-related genes. *P < 0.05.

ACOT13 along with chemokines, receptors, major histocompatibility complex genes, and immunoinhibitory and immunostimulatory genes. ACOT13 is also highly correlated with immune-related genes in many other cancers, including thymoma, liver hepatocellular carcinoma, lung adenocarcinoma, lung squamous cell carcinoma, colon adenocarcinoma, and thyroid carcinoma, suggesting that ACOT13 may affect the immune microenvironment (**Figure 9**).

Knockdown of ACOT13 promoted cell proliferation and migration

OVCAR3 is a well-established OC cell line [30]. We knocked down the expression of ACOT13 in OVCAR3 cells. RT-qPCR results showed that ACOT13 expression was downregulated in siACOT13-transfected cells compared to that in si-control cells (**Figure 10A**, $P < 0.05$). The scratch wound healing assay demonstrated that the ACOT13 knockdown promoted the migration of

OVCAR3 cells at 24 and 48 h (**Figure 10B**, **10C**, $P < 0.05$). Furthermore, significantly more colonies were formed by siACOT13-transfected OVCAR3 cells compared than by controls (**Figure 10D**, **10E**, $P < 0.05$). The percentage of migrating ACOT13 knockdown cells was higher than that of migrating si-control cells (**Figure 10F**, **10G**, $P < 0.01$). These results suggested that ACOT13 knockdown significantly increased the invasion and migration of OC cells.

Discussion

ACOT are key enzymes that affect the β-oxidation of fatty acids, with multiple effects on cellular processes such as lipid metabolism [9, 31, 32]. Imbalances in lipid metabolism also have a significant impact on tumor development. High ACOT1 expression has been observed in gastric cancer tissues, and the OS rate of patients with high ACOT1 expression is greatly reduced [33]. ACOT11 and ACOT13 are highly expressed in lung adenocarcinomas and are associated with poor prognosis [34]. In hepatocellular carcinomas, the expression of ACOT8 mRNA and the number of copies of the gene increase, and the growth of cancer cells is inhibited when ACOT8 is knocked down [35]. Correspondingly, ACOT12 expression is decreased in hepatocellular carcinoma, and downregulation of ACOT12 promotes the metastasis of hepatocellular carcinoma through epigenetic induction of TWIST2 expression [36]. To the best of our knowledge, no studies have explored the immunotherapeutic efficacy of ACOT13 in OC, and no studies have confirmed the role of ACOT13 in ovarian tumor cells using in vitro experiments. This study found that OC expressed ACOT13 at a higher level than in normal ovarian tissues. Therefore, we explored the diagnostic value of ACOT13 in OC and its effect on tumor immune infiltration.

Analysis of TCGA database revealed that ACOT13 expression was negatively correlated with FIGO grade, histological grade, lymphatic invasion, residual tumor, and tumor status. In addition, patients with OC and high ACOT13 expression had longer OS, PFS, and DSS. There was a significant independent protective effect of ACOT13 on OC in both univariate and multivariate Cox regression analyses. Based on the fact that ACOT13 expression is an important predictive factor, we developed a nomogram combining ACOT13 expression with clinical data. It was highly accurate in predicting the one-, three-, and five-year OS of patients, based on powerful ROC curves. Metastasis is one of the most important factors in the prognosis of patients affected by tumors and involves multiple steps, including the dissemination and introgression of primary tumor cells, survival of circulating tumor cells, formation of new micrometastatic colonies, and subsequent proliferation of these colonies to the point where they are clinically detectable [37]. Metastasis depends on the regulation of a complex network of intracellular and intercellular signaling cascades and remains the least understood component of cancer pathogenesis [38]. Metabolic reprogramming is a widely accepted process by which cancer cells adapt to the biosynthetic demands of metastasis [39]. ACOT13 is mainly localized in the mitochondrial matrix and is closely associated with cellular energy metabolism [40]. We believe that the expression of ACOT13 is associated with a better prognosis in patients with OC, most likely due to the role of ACOT13 in coordinating the energy metabolism of tumor cells.

Increased concentrations of long-chain fatty acyl CoA and decreased concentrations of free fatty acids were detected in the livers of ACOT13 knockout mice, which were resistant to increased glucose production in the livers of mice fed a high-fat diet [9]. Further studies have shown that ACOT13 regulates tissue concentrations of short-chain fatty acids, branched-chain amino acids, and PPP metabolites, each of which may play a role in regulating glucose homeostasis [41]. Our in vitro experiments showed that OC cells with ACOT13 knockdown were more capable of proliferation and invasion. We analyzed GO functional annotation and KEGG pathways to investigate the potential mechanism by which ACOT13 inhibits tumor development. According to the GO analysis, ACOT13 is mainly located in the mitochondrial protein complex and is closely related to several energy metabolism processes. KEGG pathway analysis also indicated that ACOT13 might inhibit epithelial cell development and mobility via various signaling pathways, including the GnRH, MAPK, and JAK-STAT signaling pathways. These findings suggest that ACOT13 plays a central role in controlling cellular energy metabolism and influences ovarian tumor cell

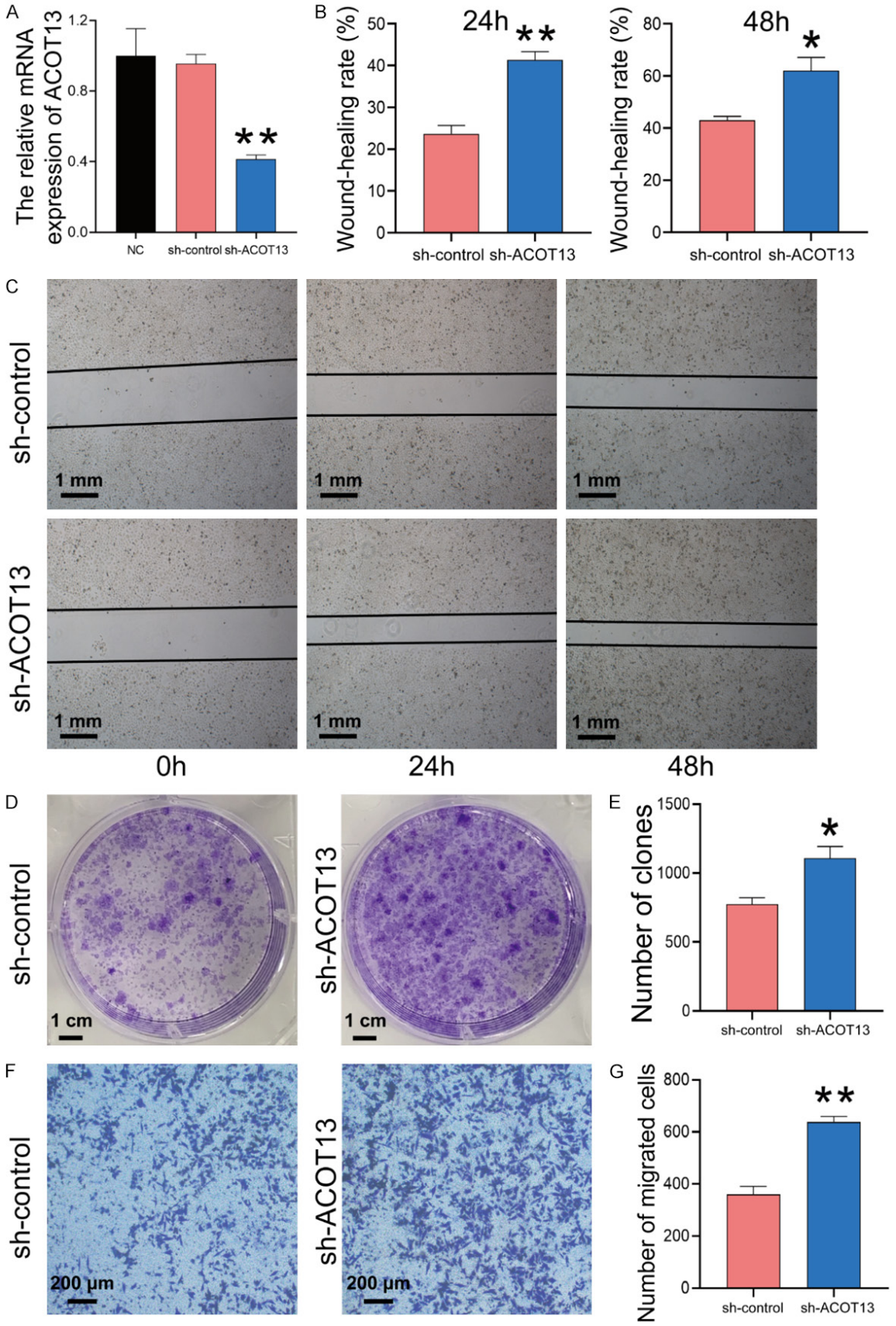
A
The relative mRNA expression of ACOT13
1.2
0.8
0.4
0.0
**
NC
sh-control
sh-ACOT13
B
Wound-healing rate (%)
24h
**
50
40
30
20
10
0
sh-control
sh-ACOT13
Wound-healing rate (%)
48h
*
80
60
40
20
0
sh-control
sh-ACOT13
C
sh-control
sh-ACOT13
1 mm
0h
24h
48h
D
sh-control
sh-ACOT13
1 cm
E
Number of clones
1500
1000
500
0
*
sh-control
sh-ACOT13
F
sh-control
sh-ACOT13
200 μm
G
Number of migrated cells
800
600
400
200
0
**
sh-control
sh-ACOT13

Figure 10. ACOT13 knockdown promoted the proliferation and migration of ovarian cancer cells. A. ACOT13 mRNA levels in OVCAR3 cells transfected with sh-control or sh-ACOT13 by reverse transcription-quantitative polymerase chain reaction (RT-qPCR). B, C. Wound healing assay of OVCAR3 cells transfected with short hairpin (sh)-control or sh-ACOT13. D, E. Colony formation in OVCAR3 cells transfected with sh-control or sh-ACOT13. F, G. Transwell assay of OVCAR3 cells transfected with sh-control or sh-ACOT13. *P < 0.05, **P < 0.01.

activity through multiple pathways. In future studies, the mechanism of action of ACOT13 in tumors should be further explored using the corresponding pathway inhibitors.

The next step in our research was to examine the role of ACOT13 in tumor immunity in detail. TIIC plays a dual role as a tumor microenvironment component that stimulates or suppresses the immune system and promotes or inhibits tumor growth [42]. Tumor prognosis is also influenced by TIIC infiltration into the tumor microenvironment [43]. Our findings suggest that ACOT13 is closely correlated with TIIC in OC and is closely associated with the infiltration of T helper, cytotoxic, and mast cells. Paclitaxel and platinum-based chemotherapeutic agents are crucial for the treatment of ovarian cancer [44]. We found that cisplatin IC50 scores were higher in patients with low ACOT13 expression, which may be one of the reasons for the poor prognosis and needs to be considered in our treatment. TMB is associated with the production of neoantigens that trigger antitumor immunity, and can be used to select patients who benefit from immune checkpoint inhibitor therapy [45]. In this study, we observed a positive correlation between ACOT13 and TMB. Therefore, immune checkpoint inhibition may be less effective in patients with low ACOT13 expression levels. To the best of our knowledge, no study has yet explored the effect of ACOT13 on the tumor immune microenvironment, and the mechanism by which ACOT13 regulates TIIC is complex and requires further research.

Immune therapies have had limited efficacy in OC, as cellular targets and mechanisms remain unclear. Therefore, a better understanding of immunotherapy response in OC is required. As a novel immune therapy, anti-PD1/PD-L1 therapy has improved the prognosis of patients with refractory solid tumors [46-50]. In this study, we investigated the correlation between ACOT13 expression and anti-PD1/PD-L1 therapy. High ACOT13 expression appears to be associated with a better CR/PR rate and a lower SD/PD rate, suggesting that high ACOT13 expression levels is associated with a better prognosis and a more effective immunotherapy response.

This study has some limitations. First, we only explored the effect of ACOT13 knockdown on the proliferation and migration of OVCAR3 cells in vitro, and additional studies are needed to elucidate the mechanism of ACOT13 in ovarian carcinogenesis. Second, the collection of clinical OC tumor tissue samples to detect ACOT13 expression and the collection of patient diagnosis and treatment information to assess the effect of immunotherapy would strengthen our conclusions. Finally, the prediction of tumor prognosis is difficult and often requires the use of multiple biomarkers; however, this does not detract from the value of ACOT13 in ovarian cancer prognosis.

Conclusions

High levels of ACOT13 expression were found in OC samples, which correlated with the FIGO classification. High ACOT13 expression negatively correlated with the degree of tumor malignancy and predicted a better prognosis. Immunotherapy resulted in better response rates in patients with high ACOT13 expression. Furthermore, ACOT13 is linked to numerous critical signaling pathways, including the regulation of energy metabolism and cell mobility. ACOT13 knockdown significantly increased invasion and migration of OVCAR3 cells. In summary, ACOT13 has excellent potential as a prognostic and immunotherapeutic biomarker of OC.

Acknowledgements

We thank Dr. Feng and Dr. Wang for their assistance with valuable instruction. This work was supported by the Natural Science Foundation of Hubei province (No. 2023AFB1084).

Disclosure of conflict of interest

None.

Address correspondence to: Nianhua Yi, Department of Women's Health Care, Maternal and Child Health Hospital of Hubei Province, Wuhan, Hubei, China. E-mail: yinianhua2000@126.com

References

[1] Momenimovahed Z, Tiznobaik A, Taheri S and Salehiniya H. Ovarian cancer in the world: epidemiology and risk factors. Int J Womens Health 2019; 11: 287-299.

[2] Gaona-Luviano P, Medina-Gaona LA and Magana-Perez K. Epidemiology of ovarian cancer. Chin Clin Oncol 2020; 9: 47.

[3] Duska LR and Kohn EC. The new classifications of ovarian, fallopian tube, and primary peritoneal cancer and their clinical implications. Ann Oncol 2017; 28: viii8-viii12.

[4] Arend R, Martinez A, Szul T and Birrer MJ. Biomarkers in ovarian cancer: to be or not to be. Cancer 2019; 125 Suppl 24: 4563-4572.

[5] Dochez V, Caillon H, Vaucel E, Dimet J, Winer N and Ducarme G. Biomarkers and algorithms for diagnosis of ovarian cancer: CA125, HE4, RMI and ROMA, a review. J Ovarian Res 2019; 12: 28.

[6] Lyu M, Li X, Shen Y, Lu J, Zhang L, Zhong S and Wang J. CircATRNL1 and circZNF608 inhibit ovarian cancer by sequestering miR-152-5p and encoding protein. Front Genet 2022; 13: 784089.

[7] Zhu C, Liu Y, Tong R and Guan J. KDF1 promoted proliferation and metastasis of epithelial ovarian cancer via Wnt/beta-catenin pathway: TCGA-based data mining and experimental validation. Front Genet 2022; 13: 808100.

[8] Morand S, Devanaboyina M, Staats H, Stanbery L and Nemunaitis J. Ovarian cancer immunotherapy and personalized medicine. Int J Mol Sci 2021; 22: 6532.

[9] Kang HW, Niepel MW, Han S, Kawano Y and Cohen DE. Thioesterase superfamily member 2/acyl-CoA thioesterase 13 (Them2/Acot13) regulates hepatic lipid and glucose metabolism. FASEB J 2012; 26: 2209-2221.

[10] Kang HW, Ozdemir C, Kawano Y, LeClair KB, Vernochet C, Kahn CR, Hagen SJ and Cohen DE. Thioesterase superfamily member 2/Acyl-CoA thioesterase 13 (Them2/Acot13) regulates adaptive thermogenesis in mice. J Biol Chem 2013; 288: 33376-33386.

[11] Kawano Y, Ersoy BA, Li Y, Nishiumi S, Yoshida M and Cohen DE. Thioesterase superfamily member 2 (Them2) and phosphatidylcholine transfer protein (PC-TP) interact to promote fatty acid oxidation and control glucose utilization. Mol Cell Biol 2014; 34: 2396-2408.

[12] Sun G, Li F, Ma X, Sun J, Jiang R, Tian Y, Han R, Li G, Wang Y, Li Z, Kang X and Li W. gga-miRNA-18b-3p inhibits intramuscular adipocytes differentiation in chicken by targeting the ACOT13 gene. Cells 2019; 8: 556.

[13] Hu X, Zhu H, Zhang X, He X and Xu X. Comprehensive analysis of pan-cancer reveals potential of ASF1B as a prognostic and immunological biomarker. Cancer Med 2021; 10: 6897-6916.

[14] Gieryng A, Pszczolkowska D, Walentynowicz KA, Rajan WD and Kaminska B. Immune microenvironment of gliomas. Lab Invest 2017; 97: 498-518.

[15] Zhang W, Wu S, Guo K, Hu Z, Peng J and Li J. Correlation and clinical significance of LC3, CD68+ microglia, CD4+ T lymphocytes, and CD8+ T lymphocytes in gliomas. Clin Neurol Neurosurg 2018; 168: 167-174.

[16] Zhu H, Hu X, Ye Y, Jian Z, Zhong Y, Gu L and Xiong X. Pan-cancer analysis of PIMREG as a biomarker for the prognostic and immunological role. Front Genet 2021; 12: 687778.

[17] Long J, Lin J, Wang A, Wu L, Zheng Y, Yang X, Wan X, Xu H, Chen S and Zhao H. PD-1/PD-L blockade in gastrointestinal cancers: lessons learned and the road toward precision immunotherapy. J Hematol Oncol 2017; 10: 146.

[18] Chhabra N and Kennedy J. A review of cancer immunotherapy toxicity: immune checkpoint inhibitors. J Med Toxicol 2021; 17: 411-424.

[19] Ito K and Murphy D. Application of ggplot2 to pharmacometric graphics. CPT Pharmacometrics Syst Pharmacol 2013; 2: e79.

[20] Hu X, Zhu H, Chen B, He X, Shen Y, Zhang X, Chen W, Liu X, Xu Y and Xu X. Tubulin alpha 1b is associated with the immune cell infiltration and the response of HCC patients to immunotherapy. Diagnostics (Basel) 2022; 12: 858.

[21] Yu T, Li D, Zeng Z, Xu X, Zhang H, Wu J, Song W and Zhu H. INSC is down-regulated in colon cancer and correlated to immune infiltration. Front Genet 2022; 13: 821826.

[22] Yu G, Wang LG, Han Y and He QY. clusterProfiler: an R package for comparing biological themes among gene clusters. OMICS 2012; 16: 284-287.

[23] Yu K, Ji Y, Liu M, Shen F, Xiong X, Gu L, Lu T, Ye Y, Feng S and He J. High expression of CKS2 predicts adverse outcomes: a potential therapeutic target for glioma. Front Immunol 2022; 13: 881453.

[24] Vasaikar SV, Straub P, Wang J and Zhang B. LinkedOmics: analyzing multi-omics data within and across 32 cancer types. Nucleic Acids Res 2018; 46: D956-D963.

[25] Hanzelmann S, Castelo R and Guinney J. GSVA: gene set variation analysis for microarray and RNA-seq data. BMC Bioinformatics 2013; 14: 7.

[26] Yoshihara K, Shahmoradgoli M, Martinez E, Vegesna R, Kim H, Torres-Garcia W, Trevino V, Shen H, Laird PW, Levine DA, Carter SL, Getz G,

Stemke-Hale K, Mills GB and Verhaak RG. Inferring tumour purity and stromal and immune cell admixture from expression data. Nat Commun 2013; 4: 2612.
[27] Feng J, Tang X, Song L, Zhou Z, Jiang Y and Huang Y. Potential biomarkers and immune characteristics of small bowel adenocarcinoma. Sci Rep 2022; 12: 16204.
[28] Tu Z, Ouyang Q, Long X, Wu L, Li J, Zhu X and Huang K. Protein disulfide-isomerase A3 is a robust prognostic biomarker for cancers and predicts the immunotherapy response effectively. Front Immunol 2022; 13: 837512.
[29] Mariathasan S, Turley SJ, Nickles D, Castiglioni A, Yuen K, Wang Y, Kadel EE III, Koeppen H, Astarita JL, Cubas R, Jhunjhunwala S, Banchereau R, Yang Y, Guan Y, Chalouni C, Ziai J, Senbabaoglu Y, Santoro S, Sheinson D, Hung J, Giltnane JM, Pierce AA, Mesh K, Lianoglou S, Riegler J, Carano RAD, Eriksson P, Hoglund M, Somarriba L, Halligan DL, van der Heijden MS, Loriot Y, Rosenberg JE, Fong L, Mellman I, Chen DS, Green M, Derleth C, Fine GD, Hegde PS, Bourgon R and Powles T. TGFbeta attenuates tumour response to PD-L1 blockade by contributing to exclusion of T cells. Nature 2018; 554: 544-548.
[30] Zhang P, Zhou X, He M, Shang Y, Tetlow AL, Godwin AK and Zeng Y. Ultrasensitive detection of circulating exosomes with a 3D-nanopatterned microfluidic chip. Nat Biomed Eng 2019; 3: 438-451.
[31] Tillander V, Alexson SEH and Cohen DE. Deactivating fatty acids: acyl-CoA thioesterase-mediated control of lipid metabolism. Trends Endocrinol Metab 2017; 28: 473-484.
[32] Cooper DE, Young PA, Klett EL and Coleman RA. Physiological consequences of compartmentalized acyl-CoA metabolism. J Biol Chem 2015; 290: 20023-20031.
[33] Wang F, Wu J, Qiu Z, Ge X, Liu X, Zhang C, Xu W, Wang F, Hua D, Qi X and Mao Y. ACOT1 expression is associated with poor prognosis in gastric adenocarcinoma. Hum Pathol 2018; 77: 35-44.
[34] Hung JY, Chiang SR, Liu KT, Tsai MJ, Huang MS, Shieh JM, Yen MC and Hsu YL. Overexpression and proliferation dependence of acyl-CoA thioesterase 11 and 13 in lung adenocarcinoma. Oncol Lett 2017; 14: 3647-3656.
[35] Hung YH, Chan YS, Chang YS, Lee KT, Hsu HP, Yen MC, Chen WC, Wang CY and Lai MD. Fatty acid metabolic enzyme acyl-CoA thioesterase 8 promotes the development of hepatocellular carcinoma. Oncol Rep 2014; 31: 2797-2803.
[36] Lu M, Zhu WW, Wang X, Tang JJ, Zhang KL, Yu GY, Shao WQ, Lin ZF, Wang SH, Lu L, Zhou J, Wang LX, Jia HL, Dong QZ, Chen JH, Lu JQ and Qin LX. ACOT12-dependent alteration of acetyl-CoA drives hepatocellular carcinoma metastasis by epigenetic induction of epithelial-mesenchymal transition. Cell Metab 2019; 29: 886-900, e885.
[37] Ding H, Li D, Chen Y, He W and Cai L. Cutaneous metastasis of ovarian cancer on 68Ga-FAPI PET/CT. Clin Nucl Med 2024; 49: 351-352.
[38] Xie F, Fu L and Zhou W. Superiority of 68Ga-FAPI-04 in delineation of soft tissue and liver metastases in chromophobe renal cell carcinoma for restaging. Clin Nucl Med 2022; 47: e758-e759.
[39] Jin Y, Jiang A, Sun L and Lu Y. Long noncoding RNA TMPO-AS1 accelerates glycolysis by regulating the miR-1270/PKM2 axis in colorectal cancer. BMC Cancer 2024; 24: 238.
[40] Bekeova C, Anderson-Pullinger L, Boye K, Boos F, Sharpadskaya Y, Herrmann JM and Seifert EL. Multiple mitochondrial thioesterases have distinct tissue and substrate specificity and CoA regulation, suggesting unique functional roles. J Biol Chem 2019; 294: 19034-19047.
[41] Imai N, Nicholls HT, Alves-Bezerra M, Li Y, Ivanova AA, Ortlund EA and Cohen DE. Up-regulation of thioesterase superfamily member 2 in skeletal muscle promotes hepatic steatosis and insulin resistance in mice. Hepatology 2022; 75: 154-169.
[42] Su J, Long W, Ma Q, Xiao K, Li Y, Xiao Q, Peng G, Yuan J and Liu Q. Identification of a tumor microenvironment-related eight-gene signature for predicting prognosis in lower-grade gliomas. Front Genet 2019; 10: 1143.
[43] Zhu H, Hu X, Feng S, Gu L, Jian Z, Zou N and Xiong X. Predictive value of PIMREG in the prognosis and response to immune checkpoint blockade of glioma patients. Front Immunol 2022; 13: 946692.
[44] Lorusso D, Raspagliesi F, Ronzulli D, Valabrega G, Colombo N, Pisano C, Cassani C, Tognon G, Tamberi S, Mangili G, Mammoliti S, De Giorgi U, Greco F, Mosconi AM, Breda E, Artioli G, Andreetta C, Casanova C, Ceccherini R, Frassoldati A, Salutari V, Giolitto S and Scambia G. Single-agent trabectedin versus physician's choice chemotherapy in patients with recurrent ovarian cancer with BRCA-mutated and/or BRCAness phenotype: a randomized phase III trial. J Clin Oncol 2024; JCO2301225.
[45] Allgauer M, Budczies J, Christopoulos P, Endris V, Lier A, Rempel E, Volckmar AL, Kirchner M, von Winterfeld M, Leichsenring J, Neumann O, Frohling S, Penzel R, Thomas M, Schirmacher P and Stenzinger A. Implementing tumor mutational burden (TMB) analysis in routine diagnostics-a primer for molecular pathologists and clinicians. Transl Lung Cancer Res 2018; 7: 703-715.

[46] Tamura R, Yoshihara K, Nakaoka H, Yachida N, Yamaguchi M, Suda K, Ishiguro T, Nishino K, Ichikawa H, Homma K, Kikuchi A, Ueda Y, Takei Y, Fujiwara H, Motoyama T, Okuda S, Wakai T, Inoue I and Enomoto T. XCL1 expression correlates with CD8-positive T cells infiltration and PD-L1 expression in squamous cell carcinoma arising from mature cystic teratoma of the ovary. Oncogene 2020; 39: 3541-3554.

[47] Dantoing E, Piton N, Salaun M, Thiberville L and Guisier F. Anti-PD1/PD-L1 immunotherapy for non-small cell lung cancer with actionable oncogenic driver mutations. Int J Mol Sci 2021; 22: 6288.

[48] Zhu P, Wang Y, Zhang W and Liu X. Anti-PD1/PD-L1 monotherapy vs standard of care in patients with recurrent or metastatic head and neck squamous cell carcinoma: a meta-analysis of randomized controlled trials. Medicine (Baltimore) 2021; 100: e24339.

[49] Schettini F and Prat A. Dissecting the biological heterogeneity of HER2-positive breast cancer. Breast 2021; 59: 339-350.

[50] Zheng Z, Guo Y and Zou CP. Oncological outcomes of addition of anti-PD1/PD-L1 to chemotherapy in the therapy of patients with advanced gastric or gastro-oesophageal junction cancer: a meta-analysis. Medicine (Baltimore) 2020; 99: e18332.

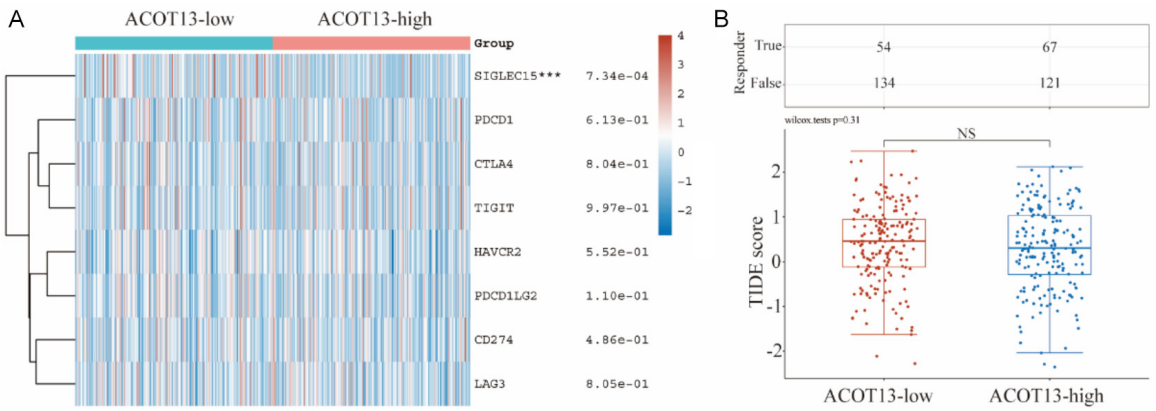

Supplementary Figure 1. Correlation between ACOT13 and immune checkpoints. A. Heatmap of immune checkpoint expression in OC with high and low ACOT13 expression. B. Different TIDE scores in OC with high and low expression of ACOT13.